APPLICATIONS OF A PEAK DETECTION CHANNEL MODEL

P. H. Siegel

Abstract - A computer model of a peak detecting magnetic recording channel has been implemented and used for channel design and performance evaluation. The model predicts raw error rate, ontrack and offtrack, as a function of linear density, run-length-limited (RLL) modulation code, write precompensation rules, and tapped-delay-line (TDL) equalizer. It assumes noise additivity and validity of linear superposition, and it bases calculations on a measured disk/electronics noise spectrum and digitized isolated transition readback signals from the data track and adjacent tracks. Details of the model are described, and illustrative applications to RLL (d,k) code selection and pulse slimming equalizer design for a specific channel are discussed.

INTRODUCTION

There are a number of signal processing options available which have the potential to increase areal density and reliability of peak detecting magnetic recording channels. Among these are modulation coding, write precompensation, and pulse slimming equalization. Assuming additivity of disk/electronics noise and adjacent track noise, and validity of linear superposition in the readback process, we have developed a model of a peak detection channel which predicts raw error rate as a function of linear density and specified signal processing. The basic methodology employed is similar to that suggested by Katz and Campbell [1] .

Novel features of the model, in addition to the implementation of a general form of the Katz-Campbell theory, include the use of Shannon theory of source coding [2] to handle arbitrary RLL (d,k) codes [3], flexible write precompensation rules, and the incorporation of a TDL equalizer for general read equalization capability.

We discuss below some of the technical aspects of the model. We then address two applications to a specific disk channel: a comparison of RLL code performance, and the selection of a minimum noise pulse slimming equalizer.

INTERSYMBOL INTERFERENCE AND CODE PATTERNS

Intersymbol interference (ISI) affects the peak position and peak amplitude of the pulse resulting from a given transition. We compute an odd ISI length L, where L is the number of bits needed to account for pulse interactions. We calculate a cubic spline fit of a digitized readback pulse from the data track, as shown in Fig. 1. Then, using linear superposition, we simulate the readback signal corresponding to each (d,k) pattern of length L having a central transition. The differentiated signal is also calculated with the spline coefficients. The position of the central peak is located by use of a Newton-Raphson iterative search for a zero-crossing in the differentiated waveform, and the central peak amplitude is then found. The model next computes the values of the differentiated waveform at the edges of the detection window corresponding to the central transition. Two types of clocking are considered: an absolute clock and a mean-centered clock. The window for the mean-centered clock is centered around the average peak position described below, and represents an approximation to the window found in a channel with a PLL (phase locked loop). The waveform derivatives at the detection window edges are required for the bit shift error rate prediction. The average peak position is found by weighting the calculated peak positions for all patterns according to the Shannon pattern probabilities, and summing. The pattern probabilities indicate the frequency of occurrence of each pattern in encoded random data for an ideal (d,k) code. Since run-lengths are uncorrelated in an ideal code, the pattern probabilities are found by taking suitable products of run-length probabilities which we compute using techniques from information theory.

Manuscript received June 16, 1982.
The author is with IBM Research Laboratory, San Jose, California 95193, U.S.A.

Write precompensation rules can be specified in order to reduce the effects of intersymbol interference. The rules are pattern dependent adjustments of the recorded transition positions: a transition is advanced or delayed by a specified amount according to the code pattern context in which it occurs.

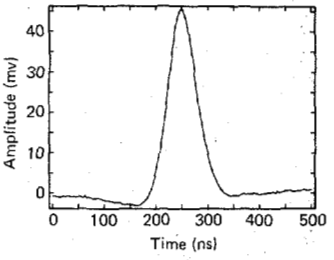

Fig. 1. Digitized isolated transition readback signal.

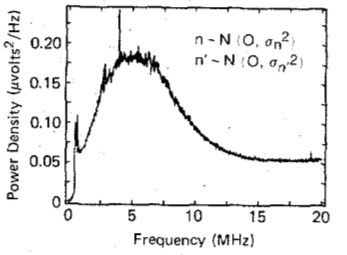

Fig. 2. Digitized disk/electronics noise power spectrum.

NOISE STATISTICS

The error rate calculation also requires a probability density function for noise and differentiated noise. For the disk/electronics noise, we digitize a noise power spectrum measured on a spectrum analyzer, as shown in Fig. 2. Normal probability plots of noise sample values measured from a dc-erased disk indicate that a Gaussian distribution fits the data out to at least three standard deviations. We take a Gaussian distribution for the disk/electronics noise, with mean zero and variance given by the numerical integral of the measured spectrum. A Gaussian distribution for the noise leads to simplifications in dealing with the differentiated noise as well. The derivative, n′, of a Gaussian noise process n is again Gaussian [4], and the power spectrum T(f) of the differentiated noise is related to that of the original noise spectrum S(f) by the expression:

$$T(f) = (2\pi f)^2 S(f). \quad (1)$$

From the digitized S(f), we then compute the variance of the differentiated noise as the numerical integral of T(f). We model the distribution of n′ as Gaussian with mean zero and with this variance.

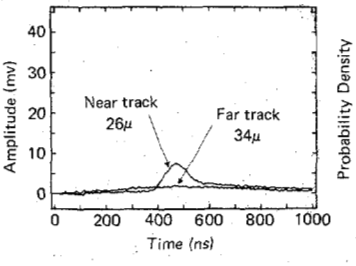

Fig. 3. Digitized adjacent track readback pulses, 4μ offtrack.

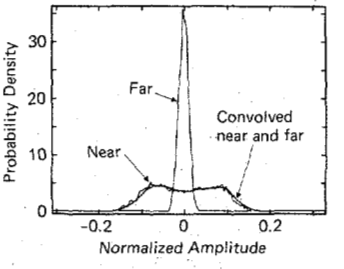

Fig. 4. Sample histograms from simulated adjacent track waveforms.

For adjacent track interference (cross-talk), we assume that side-reading of the nearest adjacent track on each side of the data track dominates the cross-talk signal. The readback signal from an isolated transition written on the adjacent track is digitized for the head position of interest. Figure 3 shows the readback pulses from the near and far adjacent tracks when the head is 4μ offtrack. Using a cubic spline fit and linear superposition, the readback waveform from several hundred bits of a pseudorandom (d,k) coded sequence is simulated and sampled up to 20 times per clock period. A histogram is made from the sample set as an estimate of the distribution density of samples from the adjacent track. If we assume no correlation between signals from different tracks, the total cross-talk density is estimated by taking the discrete

0018-9464/82/1100-1250$00.75©1982 IEEE

convolution of the histogram densities from the two tracks. Histograms from a 4μ head offset at a linear density of 18 kbpi with the (2,7) code are shown in Fig. 4, along with their convolution. The analogous calculation is then carried out for the samples of the waveform derivative. The distribution for combined disk/electronics and cross-talk noise can then be computed by discrete convolution.

ERROR RATE CALCULATION

Given that the signal has a pulse peak in the detection window W, the probability of noise-induced bit shift error is the probability that the differentiated signal plus differentiated noise waveform will fail to have a zero crossing within W:

$$Pr(\, s'(t) + n'(t) < 0 \text{ or } s'(t) + n'(t) > 0 \text{ , for } t \text{ in } W \,) \,. \quad (2)$$

Solving for this level-crossing probability exactly is a difficult mathematical problem, even when n is a Gaussian process. We use instead a convenient approximation, suggested by A. Milewski, which is a reasonably tight upper bound in the case of bandlimited noise. The probability is bounded above by the sum of the probabilities of the two events, for which simple upper bounds exist. For the first event, let t_1 be the time where the signal derivative is positive and of largest magnitude. Then,

$$Pr(\, s'(t) + n'(t) < 0 \text{ , for } t \text{ in } W \,) \le Pr(\, n'(t_1) < -s'(t_1) \,) \,. \quad (3)$$

Similarly, if t_2 is the time where the signal derivative is negative and of largest absolute value,

$$Pr(\, s'(t) + n'(t) > 0 \text{ , for } t \text{ in } W \,) \le Pr(\, n'(t_2) > -s'(t_2) \,) \,. \quad (4)$$

In practice, t_1 and t_2 have been found to lie at the detection window edges for the channels and densities studied. So, the approximations are evaluated at those points, using the waveform derivatives at the window edges and the noise distributions described above. We note that this upper bound has proven to be tighter than the approximation suggested in [1] which extrapolates the waveform derivatives at the window edges from the zero-crossing t_0 along a line of slope $s''(t_0)$. See Fig. 5.

The probability of missing bit error depends on the clip level C, which represents the minimum amplitude necessary to detect a peak in the readback signal. The probability of interest is

$$Pr(\, |s(t) + n(t)| < C, \text{ for } t \text{ in } W \,) \,. \quad (5)$$

This represents a level-crossing probability which we approximate with the simple upper bound

$$Pr(\, |s(t_0) + n(t_0)| < C \,) \,. \quad (6)$$

This probability is evaluated with the computed signal peak amplitude $s(t_0)$ and the noise distributions. See Fig. 6.

These error probability bounds may be used for approximate worst case pattern analysis. A weighted average using Shannon pattern probabilities provides an estimate of the overall error rate for encoded random data.

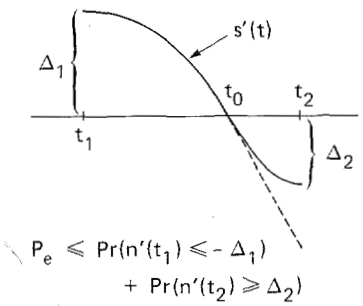

Fig. 5. Peak shift error rate approximation.

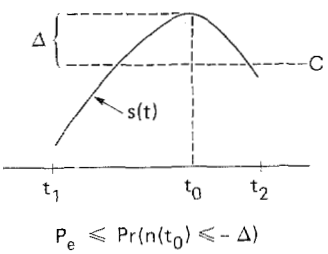

Fig. 6. Missing bit error rate approximation.

APPLICATIONS

We now discuss two applications of the model to a disk channel with a thin film head and particulate medium. Measurements were made at the inner diameter. Track pitch was 30μ.

RLL code comparison

We predicted the performance of (1,8) and (2,7) codes at three head positions - ontrack, 2μ offtrack and 4μ offtrack. The clip level was assumed to be 40% of the base-to-peak amplitude of the data track pulse. No write precompensation or pulse slimming equalization was used. The resulting error rate/linear density tradeoff curves are shown in Figs. 7 and 8. For the (1,8) code, peak shift errors dominated at densities less than 20 kbpi, while missing bits were the major error mechanism at higher densities. For the (2,7) code, however, peak shift errors were the primary determinant of error rate at all densities considered. The model indicates that at densities less than 20 kbpi, the (1,8) code has lower average error rates than the (2,7) code. At higher densities, the loss of signal amplitude degrades the (1,8) performance. In the range of error rates from 1E-12 to 1E-8, the (1,8) code provides a density advantage of slightly more than 5%. This result is consistent with the conclusions reached by Fisher and Newman in [5].

Table I shows a list of worst case patterns with L = 15 for the density 18 kbpi, as calculated by the model, along with peak shift, peak amplitude, and probability of error for ontrack operation. In general, the worst case patterns highlight features of the digitized pulses and can be used to assess the impact of peculiarities of pulse shape on error rate. Here, patterns with a minimum length run followed by a long run clearly affect the performance most severely, reflecting the pulse asymmetry.

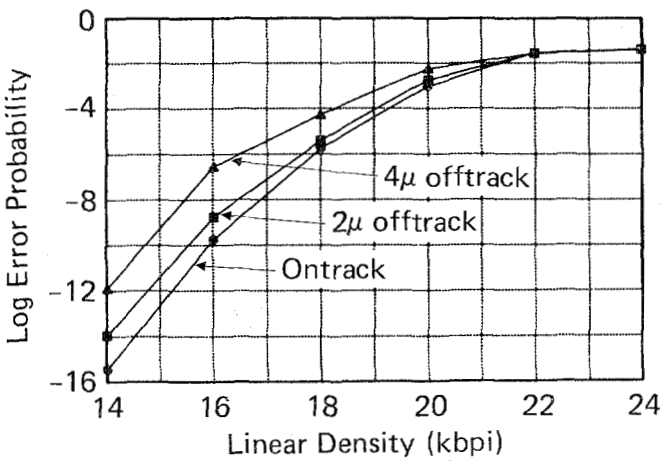

Fig. 7. Simulated performance of (1,8) code.

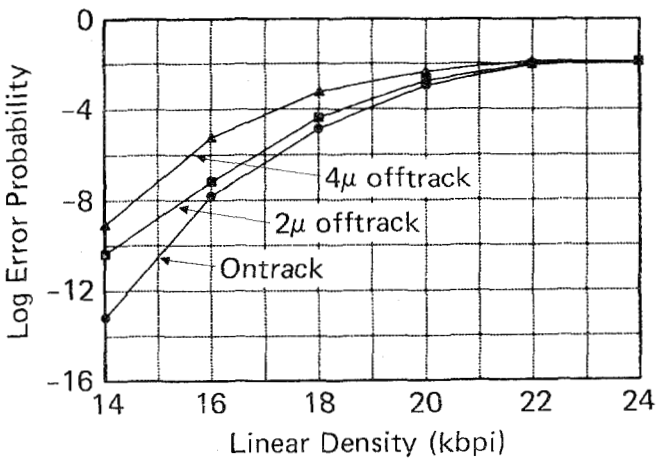

Fig. 8. Simulated performance of (2,7) code.

Peakshift (ns)	Relative Amplitude	Probability of Error	Pattern
7.1	.85	4.13E-5	100001010000101
7.0	.84	3.14E-5	010001010000101
7.1	.86	2.94E-5	100001010000100
7.2	.83	2.59E-5	000101010000101
7.0	.86	2.23E-5	010001010000100
	(1,8) code, 25.1 ns window		
5.6	.90	1.73E-3	010010010000001
5.3	.89	8.83E-4	000010010000001
5.5	.91	7.40E-4	100010010000001
5.6	.92	5.77E-4	010010010000010
5.2	.87	4.22E-4	010010010000000
	(2,7) code, 18.9 ns window		

TABLE I: Worst case patterns at 18 kbpi.

Pulse slimming equalizer evaluation

Barbosa [6] has reported on a design method for minimum noise pulse slimming equalizers. For a given channel and linear density, he constructs a one-parameter family of TDL equalizers, each of which maximizes the degree of slimming subject to a noise penalty constraint. At densities from 14 to 24 kbpi, we used the model to select the noise penalty for which the corresponding equalizer gives the smallest average ontrack error rate. The (2,7) code was used, and no cross-talk was considered. The ontrack and offtrack performance of the selected equalizer was then calculated, with cross-talk included. The results for the equalized channel with (2,7) code are shown in Fig. 9.

The conclusion based on the ontrack performance is that these equalizers can increase linear density between 10% and 20% in the range of ontrack error rates from 1E-12 to 1E-8. The equalized channel is not sensitive to small offtrack excursions, but the offtrack performance deteriorates as offtrack distance increases from 2μ to 4μ because of the enhancement of the cross-talk signal by the equalizer.

The worst case patterns were found to reflect the positions of the sidelobes of the equalized pulse. For example, at 20 kbpi, with a detection window of 17.05 ns, and with the equalized pulse shown in Fig. 10, the worst case patterns had runs of 4 zeros preceding and following the central transition, that is, 1 0 0 0 0 1 0 0 0 0 1 .

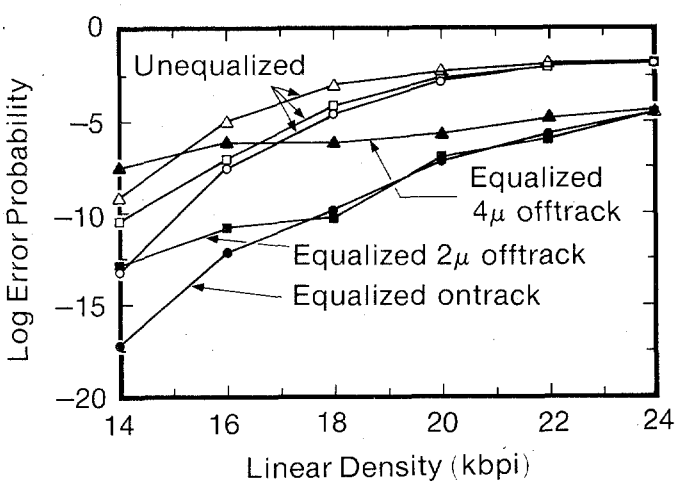

Fig. 9. Simulated performance of TDL equalizer with (2,7) code.

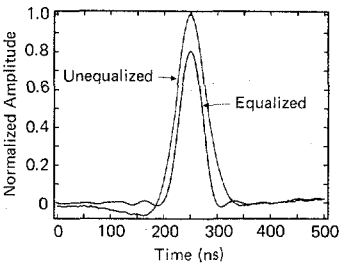

Fig. 10. Comparison of unequalized pulse and 20 kbpi equalizer pulse.

CONCLUSIONS

We have described a computer model which predicts raw error rates for a peak detecting magnetic recording channel. Offtrack performance is predicted by inclusion of adjacent track interference effects. Calculations are based on measured channel characteristics: step responses from the data and adjacent tracks, and a disk/electronics noise spectrum. The model also permits the evaluation of several signal processing options, individually and in combination: RLL code, write precompensation, and pulse slimming equalization. In addition to error rates, the model provides useful information about dominant error mechanisms and error sources both for worst case code patterns and for random coded data. Results of (d,k) code comparison and TDL equalizer evaluation for a specific disk channel were discussed.

ACKNOWLEDGMENTS

The author would like to acknowledge the early work on peak detection channel models by T. A. Schwarz.

REFERENCES

1. E. R. Katz and T. G. Campbell, "Effect of bitshift distribution on error rate in magnetic recording," IEEE Trans. Magn., vol. MAG-15, pp.1050-1053, May 1979.
2. C. E. Shannon, "A mathematical theory of communication," Bell System Tech. J., vol. 27, pp. 379-423, July 1948, and pp. 623-656, October 1948.
3. P. A. Franaszek, "Sequence-state methods for run-length-limited coding," IBM J. Res. Dev., vol. 14, pp. 376-383, July 1970.
4. D. Middleton, Introduction to Statistical Communication Theory, New York: McGraw-Hill Book Co., 1960, pp. 370-372.
5. R. D. Fisher and J. J. Newman, "Code performance and head/media interface," IEEE Trans. Magn., vol. MAG-17, pp. 1452-1454, July 1981.
6. L. C. Barbosa, "Minimum noise pulse slimmer," IEEE Trans. Magn., vol. MAG-17, pp. 3340-3342, Nov. 1981.